JPPIPA 10(Special Issue) (2024)

Jurnal Penelitian Pendidikan IPA

Journal of Research in Science Education

http://jppipa.unram.ac.id/index.php/jppipa/index

Characterisation of Tsunami Heights Affecting the Coastal Area in Ternate City

Jumaris[1*], Sigit Heru Mukti B.S[2], Sudaryatno[2]

[1] Doctoral Program of Science Geography, Universitas Gadjah Mada, Yogyakarta, Indonesia.
[2] Faculty of Geography, Universitas Gadjah Mada, Yogyakarta, Indonesia.

Received: June 7, 2024
Revised: August 16, 2024
Accepted: August 26, 2024
Published: August 31, 2024

Corresponding Author:
Jumaris
adjaris.yusra@gmail.com

DOI: 10.29303/jppipa.v10iSpecialIssue.7520

Phone*: +62…

Abstract: Ternate Island is one of the volcanic islands of the Halmahera volcanic, The Island forms an oceanic region consisting mostly of a unique double subduction tectonic deformation structure. Within this zone, the Moluccas Sea plate subducts beneath the Sangihe and Halmahera volcanic arcs. This research aims to characterise tsunami hazard to Ternate Island. The seismicity data used is combination of seismicity data from earthquake catalog by International Seismological, U.S. Geological Survey, and Meteorology, Climatology and Geophysics Agency during period 1900-2020. The main earthquake data was generated Reasenberg declustering, which previously converted earthquake magnitude for uniformity against catalogue with different data scales into moment magnitude. The tsunami source parameters in the North Maluku Sea area which are generated with a maximum magnitude of 8.5 Mw which can occur in this area are empirically capable of causing dislocations or rupture zones that reach up to 45080 km2 and the equivalent energy released in the form of seismic moments is 7.0795E+21 Nm. The maximum tsunami height at Ternate coast could be up to 3.44 meters.

Keywords: Coastal areas; Seismic activity; Tsunami; Ternate City.

Introduction

Ternate archipelago is a region dominated by complex tectonic settings, high volcanic activity and expresses the region is always vulnerable to the threat of various geological hazards. The existence of three main tectonic plates (triple Junction) that meet in this region, namely the Eurasian plate, the Indo-Australian plate and the Pacific plate converge resulting in plate collisions between each other forming a dynamic tectonic deformation structure, active volcanic arcs so that in the path of the plate meeting is the main area prone to seismicity and tsunami (BNPB, 2016; Cummins, 2017; Hamilton, 1979; Nguyen et al., 2015; Pranantyo et al., 2021; PuSGeN, 2017).

This study aims to characterise the tsunami height at the coast of Ternate Island. The North Moluccas Sea, Ternate Island and several other islands form a marine area that is mainly composed of a unique double-subduction tectonic deformation structure. Within this zone the subducting Moluccas Sea plate is thrust beneath both the Sangihe and Halmahera volcanic arcs. A collision complex occurs in opposite directions between the Sangihe arc at the margin of the Eurasian plate on its western side and the Halmahera arc as a fragment of the Philippine Sea plate on its eastern side. As a result of the convergence of the two volcanic arcs, formed the Talaud-Mayu Ridge in the Maluku Sea which stretches for at least 250 km. In addition, the zone hosts intense deformation or accretion due to convergence at the fore-arc margin (Adii et al., 2021; Hall, 1987; Hall & Smyth, 2008; McCaffrey et al., 1980; Prasetio et al., 2021; Rachman et al., 2022; Waltham et al., 2008; Widiwijayanti et al., 2003). Deformation structures such as uplift, thrust fault contact with both frontal arcs due to collision between the arcs produce characteristic

How to Cite:
Jumaris, Sigit Heru Mukti B.S., & Sudaryatno. (2024). Characterisation of Tsunami Heights Affecting the Coastal Area in Ternate City. *Jurnal Penelitian Pendidikan IPA*, *10*(SpecialIssue), 735–743. https://doi.org/10.29303/jppipa.v10iSpecialIssue.7520

shallow seismicity with magnitudes above 6.5 Mw (Hidayat et al., 2020) and low gravity anomaly values in the central Talaud Mayu Ridge zone (Danitasari et al., 2024; Utama et al., 2023; Widiwijayanti et al., 2003).

Another study describing seismicity for the period 2009 - 2019, Sabtaji (2020) presented earthquake events with a magnitude greater than or equal to 6 Mw in North Maluku province around 12% of the total events in the Indonesian region and most of the earthquake centres were in the Maluku Sea area. Similarly Hamzah et al. (2000) that in the period 1800 - 1999 there were 23 earthquake events or 17% of the total earthquake events that had occurred in Indonesia with destructive categories while the incidence of tsunamis was 32 events where 28 times the event was sourced from earthquakes and the remaining 4 times by volcanic eruptions under the sea surface. Ternate Island is one of the volcanic islands in the Halmahera volcanic arc with a dense population, and from 1800 to 2020 the island has also experienced several tsunami strikes generated by seismic activity sources in the Maluku Sea and some of them caused tsunami run-up on the coast of Ternate Island (BPS, 2021). Another database of tsunami events in the region is also not too different from the data from the Novosibirsk Tsunami Laboratory, Russia, which summarises 10 tsunami events.

This research is very important because it will provide accurate information about the tsunami potential in the Ternate archipelago, which can also be one of the efforts to prevent many victims and losses. Of course, this research is very useful for the Ternate community, stakeholders, scientists, disaster management agencies, and related scientists.

Method

This study aims to characterise the tsunami height at the coast of Ternate Island. The North Moluccas Sea, Ternate Island and several other islands form a marine area that is mainly composed of a unique double-subduction tectonic deformation structure. Within this zone the subducting Moluccas Sea plate is thrust beneath both the Sangihe and Halmahera volcanic arcs. A collision complex occurs in opposite directions between the Sangihe arc at the margin of the Eurasian plate on its western side and the Halmahera arc as a fragment of the Philippine Sea plate on its eastern side. As a result of the convergence of the two volcanic arcs, formed the Talaud-Mayu Ridge in the Maluku Sea which stretches for at least 250 km (Adii et al., 2021).

This research is very important because it will provide accurate information about the tsunami potential in the Ternate archipelago, which can also be one of the efforts to prevent many victims and losses. Of course, this research is very useful for the Ternate community, stakeholders, scientists, disaster management agencies, and related scientists.

$$m_{max} = m_{max}^{obs} + \frac{E_1(n_2) - E_1(n_1)}{\beta \exp(-n_2)} + m_{min} \exp(-n_1) \quad (1)$$

Where β is the multiplication of the value of parameter b from the G-R relation with ln 10 and n is the amount of data.

For the G-R relation, the general equation form can be written as,

$$\log 10\, n_1(m) = a + b\, mw \quad (2)$$

Equation (2) is a general linear equation with parameter a reflecting seismic parameters which depend on the period of observation data used and the wide coverage of the research area, while parameter b is a parameter which represents seismotectonic conditions such as geological environmental conditions or the level of brittleness of the underlying rock medium. The relationship with earthquake magnitude to a low b value is indicative of an area that has a high potential for large-magnitude earthquakes or destructive categories and vice versa the chance of destructive earthquakes is very small. The estimation of the b value can be done using the least square method, which can be seen in Table 1.

Table 1. Relation Model *Guttenberg-Richter (G-R)* (Gutenberg & Richter, 1944)

Earthquake Parameters		Gutenberg-Richter Relation	Number of Earthquake	Zone
Max_obs	m_max	Least square Method		
7.3 Mw	7.9 Mw	Log N(M) = 6.660 - 0.954 M	186	I
6.5 Mw	6.8 Mw	Log N(M) = 8.479 - 1.241 M	103	II
7.8 Mw	8.5 Mw	Log N(M) = 6.324 - 0.834 M	399	III

The parameters a and b from the G-R relation were used to determine the highest probability of maximum magnitude earthquake in time period t in the three grid segments in the North Maluku Sea with the Formula 3.

$$M1(t) = a/b + \log t/b \quad (3)$$

where t is a time period such as 5, 10, 50, 100, and so on.

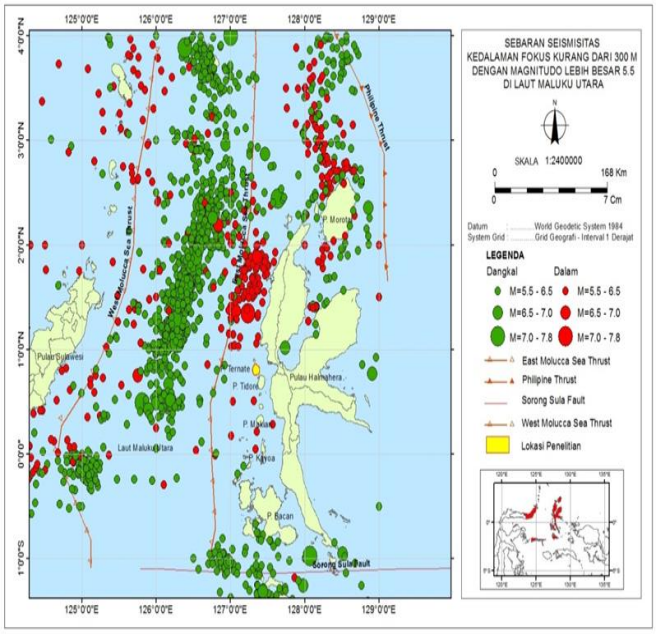

Figure 1. Map of seismicity distribution in North Maluku Sea

The probability and occurrence of earthquake recurrence (recurrence interval) is calculated based on the G-R relation and the results can be used as one of the factors of seismic activity in an area as it will show a significant correlation to the value of parameter a. Earthquake recurrence with a large magnitude can affect tsunami generation in an area or region, which can be calculated by the Formula 4.

$$T_R = \frac{1}{N(M)} \quad (4)$$

Parameterisation of the tsunami generation source is performed on the rupture plane through an empirical approach to the ratio of the seismic energy or moment (Mo) of the earthquake to the magnitude of the significant moment (Mw), the average displacement, or the area of the rupture plane that dislocates. The energy released when expressed in terms of seismic moment can be calculated based on (Kanamori, 1977) through the relationship.

$$\log M_0 = 1.5\, MW + 9.1 \quad (5)$$

The approach of relating seismic moments to the rupture zone area can reflect the tsunami generation mechanism expressed as tsunami magnitude (Mt). The relation between the tsunami magnitude (Mt) parameter and the rupture zone area can be calculated using an empirical approach with the relation.

$$\log A_r = Mt + k \quad (6)$$

where Ar is the area of the rupture zone. Meanwhile, the height of the tsunami amplitude (Htsun) in coastal waters is calculated using the equation.

$$Htsun = [Mw - 0.213 \log R - 9.2019 \prod Z_0/Z_1]^{0.25} \quad (7)$$

where R = distance of the tsunami generation source to the location of the observation point, Z0 = depth of the tsunami generation source from mean sea level, and Z1 = depth of the observation point in coastal waters. Similarly, the tsunami height can be determined by the relation Htsun *= 2 Htsun.

Result and Discussion

The distribution of tsunamis on the coast of Ternate Island is strongly influenced by seismotectonic conditions in the North Maluku Sea. As shown in Figure 1, the distribution of seismicity points reflects the relatively high level of seismic activity in the region. The distribution of seismicity is illustrated from the compilation of catalogue data with earthquake magnitude ≤ 5.5 Mw and epicentral depth 300 Km with the period of occurrence from 1900 to 2020. The distribution of shallow earthquake hypocentres (≤70 Km) can be found under the Talaud Mayu ridge with the tendency for the epicentre points to form clusters that parallel follow the zone area in the North Maluku Sea and also around Bacan Island.

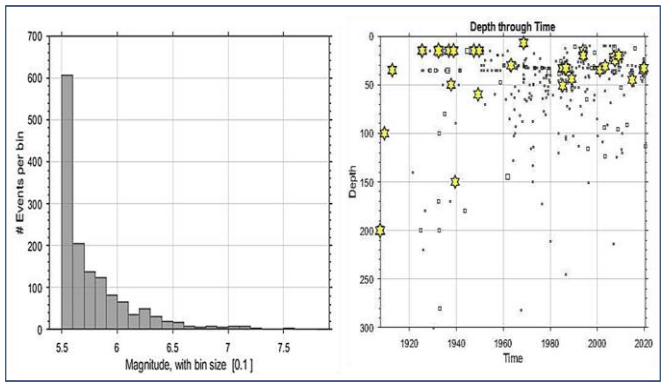

Figure 2. Earthquake profile for magnitude ≥ 5.5 and central depth ≤ 300 Km in the North Maluku Sea.

Both forms of earthquake clusters are generally formed and affected by the enlargement structure in the Collision complex and the active Sorong - Bacan fault structure. In addition, there is also a distribution of earthquake depths exceeding 70 Km also seen spreading randomly to the north of Morotai island near the boundary of the Philippine megathrust. There is also a cluster of deep category earthquakes in the Halmahera subduction zone or between the Halmahera island arc

and the Halamahera trench with intermittent occurrences of earthquakes with magnitudes greater than 7.0. Figure 2 shows a profile of large magnitude earthquakes dominated by epicentre depths of less than 70 km as well as frequency of occurrence.

The presence of the Talaud Mayu central ridge creates a seedbed of very active seismicity consisting of a distribution of large-magnitude earthquake epicenters with shallow epicenter depths. This distribution situation encloses a collision complex zone that expresses the tectonic complexity in the North Maluku Sea and can potentially be a source of tsunami hazard to the surrounding islands including Ternate island.

An earthquake event with a magnitude of ≥ 7.0 (yellow star symbol in figure 2) and a shallow epicenter depth is one of the factors that has the potential to generate tsunamis because it has a significant probability of causing large dislocations in the fault zone or in the collision between plates.

In the history of seismicity in the North Maluku Sea, at least two tsunami events have been recorded between 1980 to 2020, namely the tsunami events in November 2014 and July 2019, which were triggered by the release of energy equivalent to a large earthquake magnitude with each source mechanism type of thrust fault and splay fault. Figure 3 is a figure showing the parameters of the earthquake focal mechanism affecting the thrust fault/reverse fault and oblique fault and the magnification is initiated as a controlling parameter for several earthquake events in the Maluku Sea region.

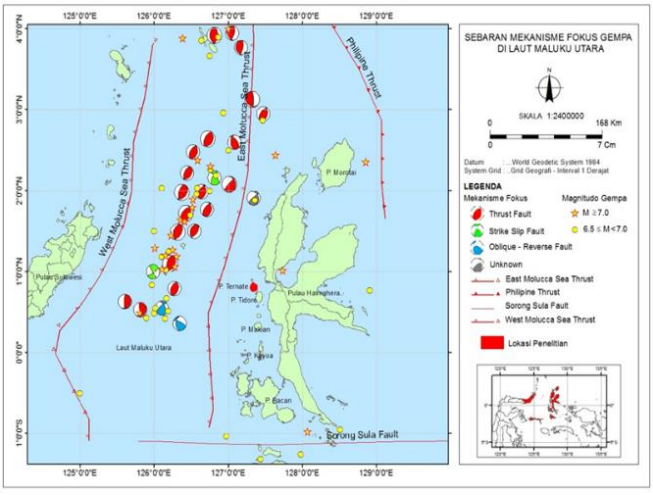

Figure 3. Distribution of earthquake focus mechanisms in the North Maluku Sea

The spherical distribution of the focal mechanism in Figure 3 above illustrates the intense deformation that affects the expansion of the upward fault zone on the Talaud-Mayu ridge with an orientation trend towards the North-Northeast and South-Southwest and aligns with the East and West boundary lines of the North Maluku Sea thrust. Its relation to the seismotectonic situation has been revealed in the research (Fazriati et al., 2022; Fazriati et al., 2023; Prasetio et al., 2021) ,that the main structural pattern occurs in the Talaud-Mayu area, 2021) that the main structural pattern that occurs is dominant through the thrust fault mechanism that is elongated in the middle of the Maluku Sea with a Northeast-Southwest orientation, and other researchers Hamilton (1974) suggested the existence of a thrust fault type mechanism concentrated in the Maluku Sea plate under the Talaud Mayu ridge with the expression of the distribution of high-density earthquake centers along the ridge. Similarly, in the regional aspect, the pressure influence of the annual convergent movement between the Philippine plate and the Sunda plate relative to each double subduction boundary of the Moluccas Sea plate is increasingly squeezed and sinked.

Estimated b parameter values and earthquake recurrence interval

The recurrence of seismic activity over a certain time span in the North Maluku sea area is predicted using a probability function approach such as a relation function which states the relationship between the frequency of earthquake events and their magnitude, known as the Getenberg-Richter (G-R) relation (Deswanti et al., 2022; Meidji et al., 2023; Sanny et al., 2023). In this function, priority is given to determining the coefficient b value and a value estimated using the least squares method for each specific regional division or each grid segment. Previously, the main earthquake data was separated from its aftershocks by filtering (Reasenberg declustering) using the Zmap 7.1 application program.

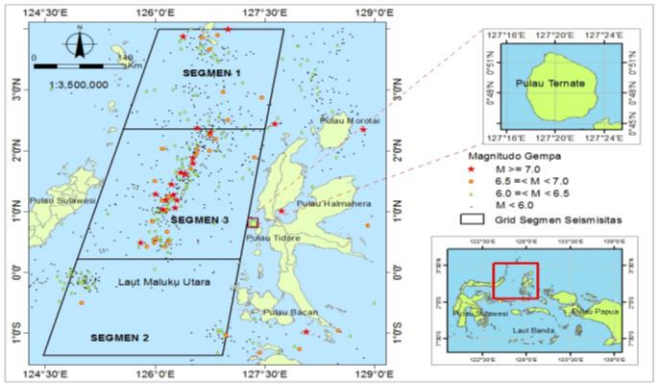

Figure 4. Grid division of research segments and distribution of main earthquakes in the North Maluku Sea

The existence of the Talaud Mayu ridge in the North Maluku Sea has become a place for the distribution of intense earthquakes with a magnitude greater than or equal to 4 (M ≥ 4, Mc = 4.9) with seismotectonic parameters namely b = 1.16 ± 0.02 but the

value of b is more dominant within the limits b value ≤ 1.2 (dotted red circle) as seen in Figure 4. These results are also significantly correlated when compared with the estimates of each b value for the three grid segments of the study where the results vary in value between 0.834 – 1.241 (seen in the table 1).

The range of values is comparable to the b value of grid segment 3 which spatially shows a higher density of earthquake points than the other two segments. In addition, the value of 0.834 has also become an active seismic distribution area dominated by the magnitude of ≥ 7.0 Mw as seen in Figure 5. The processing results of the b parameter value in each segment are relatively different, it depends on the review of the segment area between one another and the influence of seismotectonic medium conditions or the degree of rock fragility.

Differences in parameter b values also indicate the degree of vulnerability to intense seismic deformation in a particular area. A relatively low b value indicates high vulnerability to large magnitude and potentially damaging earthquakes. Likewise, in relation to the vulnerability of tsunami hazards in the North Maluku Sea, the potential for a tsunami to be generated by a large earthquake magnitude is possible to form in segment 1 and segment 3 only, as determined by equation (1) in grid segment 3 the maximum magnitude can reach 8.5 Mw then followed by grid segment 1 which can also reach a maximum magnitude of 7.9 Mw (as seen in Table 1).

As noted in the catalogue (BMKG, 2019), between 1800 and 2020, segment 3 as an area with high potential to represent tsunami events in the North Maluku Sea region has triggered at least 7 tsunami events with tsunami magnitudes (Iida) varying from -1.3 to 3.2. Illustrating the profiles of the seven tsunami events, there are tsunami events, especially those that occurred in 1846 and 2014, which are thought to be two identical tsunami events with spatial source coordinates showing relatively close locations.

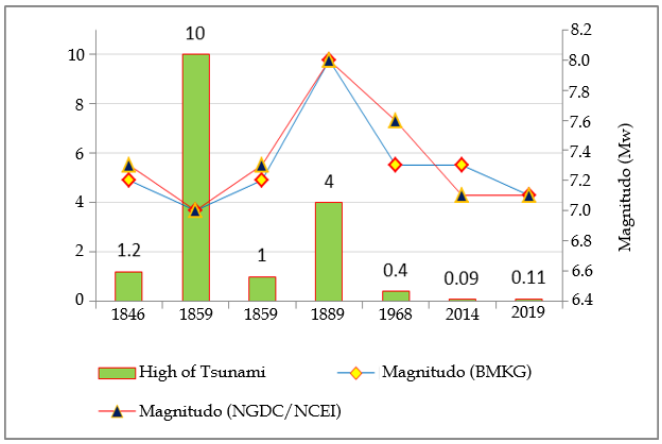

Figure 5. Profile of tsunami events from 1846 to 2020 in the North Maluku Sea.

The earthquake recurrence approach can also be seen as a parameter of tsunami hazard vulnerability in an area by comparing the average recurrence rate of large-magnitude earthquake events that can be exceeded at least once in a certain time period. The probability of earthquake recurrence (return period) appears to be directly proportional to the level of seismicity of a region, which is represented by the value of the parameter a of the G-R relation (Akhsan et al., 2022; Yasper et al., 2023).

For the probability level of recurrence of an earthquake with a large magnitude that has the potential to trigger a tsunami in the North Maluku Sea area for each of the three grid segments of the research area, it is calculated using the G-R relationship using equation 4. In the G-R relationship, the probability and characteristics of earthquake recurrence with a magnitude of 6.8 Mw up to 7.5 Mw has a fairly high chance of causing seabed dislocations or rupture areas and is likely to form in grid segment 3 in the next 20 to 100 years and in full can be seen in Table 2.

Table 2. Probability and recurrence of earthquakes from the G-R relationship in grid segment 3

Mw	G-R Relation	Probability Occurrence at year (%)					T_R
	$N_1(M)$	t = 5	t = 10	t = 20	t = 50	t = 100	(th)
6.8	0.047	20.9	37.5	61.0	90.5	99.1	21
6.9	0.039	17.6	32.2	54.0	85.6	97.9	26
7	0.032	14.8	27.4	47.3	79.8	95.9	31
7.1	0.026	12.4	23.2	41.0	73.3	92.9	38
7.3	0.018	8.6	16.5	30.2	59.3	83.5	56
7.5	0.012	5.9	11.5	21.7	45.8	70.6	82
7.8	0.007	3.4	6.7	12.9	29.1	49.8	145
8	0.005	2.3	4.6	8.9	20.9	37.4	213
8.1	0.004	1.9	3.8	7.4	17.6	32.1	259
8.5	0.002	0.9	1.8	3.5	8.6	16.4	557

Table 3. Probability and recurrence of earthquakes from the G-R relationship in grid segment 1

Mw	G-R Relation	Probability Occurrence at year (%)					T_R (yr)
	N_1(M)	t = 5	t = 10	t = 20	t = 50	t = 100	
6.8	0.018	8.4	16.1	29.6	58.3	82.6	57
6.9	0.014	6.8	13.1	24.5	50.5	75.5	71
7	0.011	5.5	10.7	20.2	43.1	67.7	89
7.1	0.009	4.4	8.7	16.6	36.4	59.6	110
7.3	0.006	2.9	5.7	11.0	25.3	44.2	171
7.5	0.004	1.9	3.7	7.3	17.2	31.4	266
7.8	0.002	1.0	1.9	3.8	9.3	17.7	514
8	0.001	0.6	1.2	2.5	6.1	11.8	797

Likewise, with grid segment 1, the probability and return period of earthquakes as in Table 5, earthquake repetitions that are likely to occur for the next 50 to 100 years are earthquakes with magnitudes of 6.8 Mw to 7.1 Mw determined through the G-R relation.

Table 4. Empirical parameters of the rupture field in the North Maluku Sea area.

M	Mo (Nm)	D_rt(m)	L (Km)	A (Km2)	Mt	Mt*	*RunUp* (meter)	*RunUp** (meter)
6.9	2.8184E+19	0.903441	35	945.34	-0.4	-0.4	0.8	0.8
7.1	5.6234E+19	1.111988	46	1532.45	0.1	0.1	1.1	1.1
7.3	1.1220E+20	1.368674	62	2484.20	0.4	0.6	1.3	1.5
7.5	2.2387E+20	1.684612	82	4027.04	0.8	1.1	1.7	2.1
7.8	6.3096E+20	2.300382	125	8311.63	1.3	1.9	2.5	3.7
8.1	1.7783E+21	3.141232	191	17154.82	1.9	2.7	3.7	6.5
8.3	3.5481E+21	3.866340	253	27809.04	2.2	3.2	4.6	9.2
8.5	7.0795E+21	4.758828	336	45080.22	2.8	3.7	7.0	13

The smaller magnitude of the earthquake in grid segment 3 or ≤ 7.5 Mw with a relatively short TR return period with an equivalent seismic moment of 2.2387E + 20 Nm is thought to capable of being the triggering energy for the tsunami event in the North Maluku Sea. In grid segment 3, the earthquake return period is also shorter at 56 - 82 years and the probability of occurrence is quite high at 59.3% - 70.6%. The relationship with the recurrence of a potentially large tsunami event in the segment is indicated by the presence of intense deformation through an earthquake mechanism with a magnitude of around 7.3 to 7.5 Mw.

As in the case of the recorded tsunami events in the North Maluku Sea, tsunamis are generally triggered by earthquakes of magnitude above 7 Mw focused on the Talaud Mayu ridge with a thrust fault focal mechanism in grid segment 3, while in grid segment 1 and grid segment 2 there are no traces of tsunami events in the available catalogues. In addition to this, the probability of tsunami generation in grid segment 1 also remains high, especially since within this segment the distribution of earthquakes with shallow focal depths and earthquake magnitudes above 6.8 Mw can form in a zone that is classified as a continuation of the northward part of the Talaud Mayu ridge.

Tsunami Height Estimation in the Ternate Coastline

The surface area of the rupture area can be assumed to be an empirical parameter of the tsunami generation source that depends on the geometry of the rupture plane length, width and magnitude of the slip displacement over the extent of the rupture zone. The length of the rupture surface dislocation zone, if it can reach ≥ 1000 km, tends to express extreme megatsunamiigenic generation while the size of the rupture zone plane contributes linearly to the tsunami magnitude and *the tsunami run-up*. Tsunami triggering parameters in the North Maluku Sea, especially in zone 3 and zone 1, can be estimated empirically by determining the length of the rupture zone surface and then comparing it to the seismic moment as a reflection of the level of energy release with magnitudes from 6.9 Mw to 8.5 Mw. The empirical estimation was carried out using the Thingbaijam formula and the calculated rupture zone surface plane length can reach 336 Km and the maximum rupture zone area is about 45080 Km2 with tsunami magnitude equivalence (without units) between -0.4 and 2.8 and can be seen in Table 5.

The range of earthquake magnitudes in Table 5 are parameters of earthquakes that are categorised as destructive and contain the equivalent energy to trigger a tsunami and the relationship between earthquake magnitude and tsunami run-up with reference to Iida's run-up formulation (Kulikov et al., 2005) an earthquake magnitude of 8.5 Mw is equivalent to a tsunami magnitude of 3.7 which can produce a tsunami run-up height of 13 meters on the coast of Ternate Island. In another form the tsunami magnitude can also be assumed to be a function of the area of the dislocation

field formed as seen in Table 7, a rupture geometry area of about 45080 Km² is omparable to a tsunami magnitude of 2.8 and generates a tsunami height of 7.0 meters.

Table 5. Distribution of tsunami height parameters in the North Maluku Sea area.

Mw	Mt	AmpTsun (min – max)	Htsun (min – max)	Ht_sig(m)	Stdv
6.9	-0.4	0.02 m – 0.04 m	0.04 m – 0.08 m	0.06	0.011
7.1	0.1	0.03 m – 0.07 m	0.06 m – 0.14 m	0.09	0.017
7.3	0.4	0.04 m – 0.11 m	0.08 m – 0.22 m	0.15	0.028
7.5	0.8	0.07 m – 0.17 m	0.14 m – 0.34 m	0.24	0.043
7.8	1.3	0.13 m – 0.34 m	0.26 m – 0.68 m	0.47	0.086
8.1	1.9	0.26 m – 0.68 m	0.52 m – 1.36 m	0.94	0.172
8.3	2.2	0.42 m – 1.09 m	0.84 m – 2.18 m	1.50	0.273
8.5	2.8	0.66 m – 1.72 m	1.32 m – 3.44 m	2.37	0.433

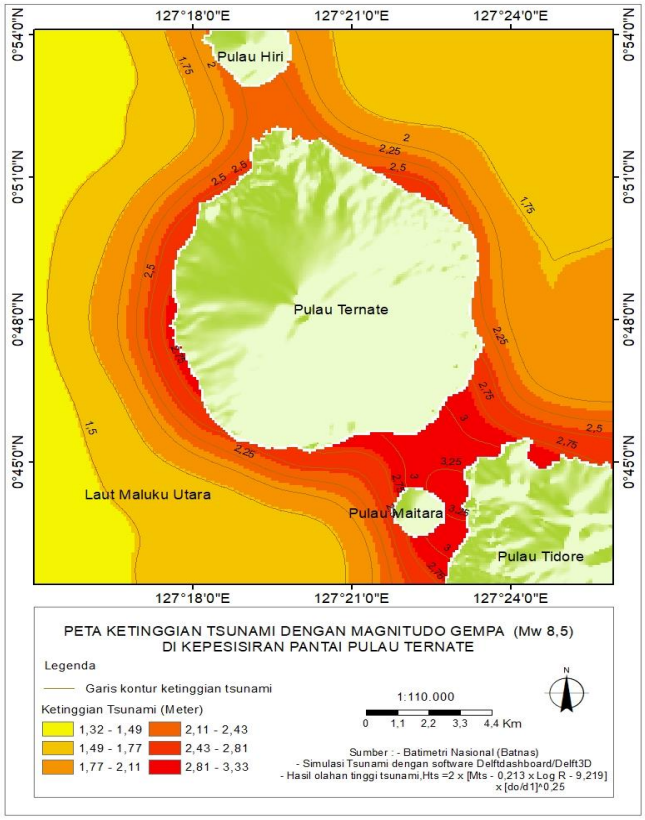

Figure 6. Distribution of tsunami heights on the coast of Ternate Island

In relation to the prediction of tsunami run-up on the coast of Ternate Island, it is carried out by referring to the spatial distribution of the maximum tsunami amplitude resulting from numerical model calculations using the Delftdashboard/Delft3D application programme and then developed into the tsunami height equation in equation (7). The distribution of tsunami height on the coast of Ternate is an equation whose parameters are determined from the mechanism of the earthquake that occurred on 14 November 2014 and generated a tsunami with a height of 0.09 m (BMKG, 2021) on the coast of Ternate. The spatial distribution of tsunami heights obtained from equation (7) can be seen in Figure 6. In addition, the height of the tsunami that formed and reached the coast of Ternate Beach can be expressed in tsunami magnitude (without units) from -0.4 to 2.8, which is equivalent to a height of 0.04 meters to 3.44 meters. These heights also represent the average (significant) height from 0.06 meters to 2.37 meters.

The distribution of tsunami height on the coast of Ternate Island, as in Figure 6, shows the level of vulnerability to tsunami danger with the threat of tsunami wave height reaching 3.44 meters. The orange gradient in the image represents the height of the tsunami which exceeded 2.43 meters and was distributed relatively uniformly around the coastline of Ternate Island. Beaches that experienced significant exposure to tsunami wave heights include beaches located to the south and southeast of Ternate Island, which administratively are in the South Ternate and Central Ternate Districts. The coastal situation of the two sub-districts is also directly connected to the effects of coastal morphography from Maitara Island and Tidore Island which are to the southeast. The east, north and west coasts of Ternate Island are dominated by the morphological appearance of rocky beaches and steep walls and some of them are still in the form of forest plantations or some of these lands have also been used as beach tourism areas (Fitriani et al., 2021). The sea that is located between the coasts of the three islands is waters with a more diverse, complex seabed topographic situation and has a relatively shallow depth (Hasyim et al., 2023). On the coast of Ternate Island, especially areas that have relatively flat relief, the shape of the beach configuration is relatively straight, slightly sloping and has been occupied as a strategic area for the Ternate urban area as well as residential areas with high density so that the areas in these two sub-districts have the potential for high vulnerability to tsunami hazards.

Conclusion

The tsunami source parameters in the North Maluku Sea area which are generated with a maximum

magnitude of 8.5 Mw which can occur in this area are empirically capable of causing dislocations or rupture zones that reach up to 45080 km2 and the equivalent energy released in the form of seismic moments is 7.0795E+21 Nm. The probability of a tsunami that can form on the coast of Ternate Island is capable of reaching a maximum height of 3.44 meters with a tsunami magnitude of 2.8 (without units) and originates from a tsunami generation source which is a dislocation area which can be caused by a thrust fault type earthquake source mechanism and tends to form in the midles of the Talaud Mayu ridge.

Acknowledgments
We would like to express our deepest gratitude to the promoter team and the parties who have helped the completion of this research.

Author Contributions
This manuscript was written by Jumaris as creator and validator, while Sigit Heru M. and Sudaryatno served as the supervisory team.

Funding
This research received no external funding.

Conflicts of Interest
During the work and completion of this manuscript, never once experienced a conflict of interest.

References

Adii, J., Kusumawati, D., Falevi, C., & Sahara, D. P. (2021). Maluku Sea Plate Faulting Regime Analysis: A Preliminary Study. *IOP Conference Series: Earth and Environmental Science*, *873*. https://doi.org/10.1088/1755-1315/873/1/012100

Akhsan, H., Romadoni, M., & Ariska, M. (2022). Prediction of Extreme Temperature in South Sumatra and Its Applications at The End of The 21st Century. *Jurnal Penelitian Pendidikan IPA*, *8*(2), 925–931. https://doi.org/10.29303/jppipa.v8i2.1363

BMKG. (2019). *Katalog Tsunami Indonesia Tahun 416-2018. Pusat Gempa Bumi dan Tsunami Kedeputian Bidang Geofisika*. Retrieved from https://cdn.bmkg.go.id/Web/Katalog-Tsunami-Indonesia-pertahun-416-2018.pdf

BMKG. (2021). *Katalog Gempa Bumi*. Retrieved from https://geof.bmkg.go.id/webdc3/

BNPB. (2016). *Indeks Risiko Bencana Indonesia*. BNPB. Retrieved from https://inarisk.bnpb.go.id/irbi

BPS, K. T. (2021). *Kota Ternate Dalam Angka*. BPS Kota Ternate. Retrieved from https://ternatekota.bps.go.id/id/publication/2021/02/26/00b68152f9fd66b4303d883e/kota-ternate-dalam-angka-2021.html

Cummins, P. R. (2017). Geohazards in Indonesia: Earth science for disaster risk reduction - introduction. *Geological Society Special Publication*, *441*(1), 1–7. https://doi.org/10.1144/SP441.11

Danitasari, F., Ryan, M., Handoko, D., & Pramuwardani, I. (2024). Improving Accuracy of Daily Weather Forecast Model at Soekarno-Hatta Airport Using BILSTM with SMOTE and ADASYN. *Jurnal Penelitian Pendidikan IPA*, *10*(1), 179–193. https://doi.org/10.29303/jppipa.v10i1.5906

Deswanti, B., Marzuki, M., Muharsyah, R., Yusnaini, H., & Ramadhan, R. (2022). Influence of Weather Conditions on COVID-19 Case in Several Regions of Indonesia. *Jurnal Penelitian Pendidikan IPA*, *8*(3), 1538–1547. https://doi.org/10.29303/jppipa.v8i3.1851

Fazriati, E., Azhari, M. R., Hakam, A., Utama, W., & Rosandi, Y. (2023). Horizontal to Vertical Spectral Ratio (HVSR) Analysis of the Passive Seismic Data on Alluvial Lithology: An Example from Bandung Basin Rim. *Jurnal Penelitian Pendidikan IPA*, *9*(1), 402–411. https://doi.org/10.29303/jppipa.v9i1.2962

Fazriati, E., Purnama, A., Algifari, G. A., Muslimah, I. S. A., Sumanto, F. H. P., Kirana, K. H., Susanto, K., A., B., A., B., A., M., Behrens, J., Costa, A., Davies, G., & Thio, H. K. (2022). Cross-Section Resistivity Detection of Tree (Swietenia Magahoni and Gmelina) Using ERT Method. *Jurnal Penelitian Pendidikan IPA*, *8*(1), 39–44. https://doi.org/0.29303/jppipa.v8i1.965

Fitriani, D., Utami, W., Kirana, K. H., Agustine, E., & Zulaikah, S. (2021). Magnetic Signatures on River Sediments and Agricultural Soils as Proxy Indicators of Anthropogenic-derived Pollution (Case Study: Cikijing River, Rancaekek, West Java). *Jurnal Penelitian Pendidikan IPA*, *7*(3), 381–387. https://doi.org/10.29303/jppipa.v7i3.697

Gutenberg, B., & Richter, C. F. (1944). Frequency of earthquakes in California*. *Bulletin of the Seismological Society of America*, *34*(4), 185–188. https://doi.org/10.1785/BSSA0340040185

Hall, R. (1987). Plate boundary evolution in the Halmahera region, Indonesia. *Tectonophysics*, *144*(4), 337–352. https://doi.org/10.1016/0040-1951(87)90301-5

Hall, R., & Smyth, H. R. (2008). Cenozoic arc processes in Indonesia: Identification of the key influences on the stratigraphic record in active volcanic arcs. *Special Paper of the Geological Society of America*, *436*(03), 27–54. https://doi.org/10.1130/2008.2436(03)

Hamilton, W. (1974). *Earthquake Map of The Indonesian Region*. U.S Geological Survey.

Hamilton, W. (1979). *Tectonics of the Indonesian Region*. United States Government Printing Office. https://doi.org/10.7186/bgsm06197301

Hamzah, L., Puspito, N. T., & Imamura, F. (2000). Tsunami Catalog and Zones in Indonesia. *Journal of Natural Disaster Science*, *22*(1), 25–43. https://doi.org/10.2328/jnds.22.25

Hasyim, A., Yusal, M. S., Syamsuri, S., & Alang, H. (2023). Meiobenthos Community as a Description of Environmental Changes at Losari Beach Makassar. *Jurnal Penelitian Pendidikan IPA*, *9*(11), 10308–10316. https://doi.org/10.29303/jppipa.v9i11.3773

Hidayat, A., Marfai, M. A., & Hadmoko, D. S. (2020). Eruption on Indonesia's volcanic islands: A review of potential hazards, fatalities, and management. *IOP Conference Series: Earth and Environmental Science*, *485*(1), 12061. https://doi.org/10.1088/1755-1315/485/1/012061

Kanamori, H. (1977). The energy release in great earthquakes. *Journal of Geophysical Research*, *82*(20), 2981–2987. https://doi.org/10.1029/jb082i020p02981

Kulikov, E. A., Rabinovich, A. B., & Thomson, R. E. (2005). Estimation of tsunami risk for the coasts of Peru and Northern Chile. *Natural Hazards*, *35*(2), 185–209. https://doi.org/10.1007/s11069-004-4809-3

McCaffrey, R., Silver, E. A., & Raitt, R. W. (1980). Crustal structure of the Molucca Sea collision zone, Indonesia. The tectonic and geologic evolution of Southeast Asian seas and islands. *The Tectonic and Geologic Evolution of Southeast Asian Seas and Islands*. Retrieved from https://earthjay.com/earthquakes/20170408_philipines/mccaffrey_etal_1980_molucca_sea_tectonics.pdf

Meidji, I. U., Jatnika, J., Samatowa, L., Ramadani, A. I. W. S., Ramdhan, M., Efendi, H. A., & Jayadi, H. (2023). Analyzing Seismicity Pattern of the Gorontalo Region and Its Surroundings in the Form of Hypocenter Relocation Using Double Difference Method. *Jurnal Penelitian Pendidikan IPA*, *9*(10), 8581–8587. https://doi.org/10.29303/jppipa.v9i10.5400

Nguyen, N., Griffin, J., Cipta, A., & Cummins, P. R. (2015). *Indonesia's Historical Earthquakes: Modelled examples for improving the national hazard map*. Australian Goverment: Geoscience Australia. https://doi.org/10.11636/record.2015.023

Pranantyo, I. R., Heidarzadeh, M., & Cummins, P. R. (2021). Complex tsunami hazards in eastern Indonesia from seismic and non-seismic sources: Deterministic modelling based on historical and modern data. *Geoscience Letters*, *8*(20), 1–16. https://doi.org/10.1186/s40562-021-00190-y

Prasetio, A. D., Hasib, M., Amran, A., Syuhada, F., F., D., N., C., & Anggono, T. (2021). Local seismotectonic analysis of the. *Geoscience Letters*, *8*(1). https://doi.org/10.1186/s40562-021-00200-z

PuSGeN. (2017). *Peta Sumber Dan Bahaya Gempa Indonesia Tahun 2017*. Pusat Litbang Perumahan dan Permukiman Kementerian PUPR. Retrieved from https://docslib.org/doc/3199330/peta-sumber-dan-bahaya-gempa-indonesia-tahun-2017

Rachman, G., Santosa, B. J., Nugraha, A. D., Rohadi, S., Rosalia, S., Zulfakriza, Z., & Afif, H. (2022). Seismic Structure Beneath the Molucca Sea Collision Zone from Travel Time Tomography Based on Local and Regional BMKG Networks. *Applied Sciences (Switzerland)*, *12*(20). https://doi.org/10.3390/app122010520

Sabtaji, A. (2020). Statistik kejadian gempa bumi tektonik tiap provinsi di wilayah Indonesia selama 11 tahun pengamatan (2009-2019). *Buletin Meteorologi, Klimatologi, Dan Geofisika*, *1*(7), 31–46. Retrieved from https://shorturl.asia/eczFk

Sanny, T. A., Asrib, M. L., & Insani, A. Z. M. (2023). Soil Characterization using the Electrical Resistivity Tomography (ERT) Approach on Non-Typical Land of Ipomoea Batatas. *Jurnal Penelitian Pendidikan IPA*. https://doi.org/10.29303/jppipa.v9i8.4653

Utama, W., Garini, S. A., Hutapea, M. C., Putra, D. P. N., Warnana, D. D., & Lestari, W. (2023). Effect of Geometry and Number of Seismic Stations on Micro-Earthquake (MEQ) Hypocenters in Geothermal Fields. *Jurnal Penelitian Pendidikan IPA*, *9*(10), 8114–8123. https://doi.org/10.29303/jppipa.v9i10.3742

Waltham, D., Hall, R., Smyth, H. R., & Ebinger, C. J. (2008). *Basin formation by volcanic arc loading*. Geological Society of America. https://doi.org/10.1130/2008.2436(02)

Widiwijayanti, C., Mikhailov, V., Diament, M., Deplus, C., Louat, R., Tikhotsky, S., & Gvishiani, A. (2003). Structure and evolution of the Molucca Sea area: Constraints based on interpretation of a combined sea-surface and satellite gravity dataset. *Earth and Planetary Science Letters*, *215*(1–2), 135–150. https://doi.org/10.1016/S0012-821X(03)00416-3

Yasper, A., Handoko, D., Putra, M., Aliwarga, H. K., & Rosid, M. S. R. (2023). Hyperparameters Optimization in XGBoost Model for Rainfall Estimation: A Case Study in Pontianak City. *Jurnal Penelitian Pendidikan IPA*, *9*(9), 7113–7121. https://doi.org/10.29303/jppipa.v9i9.3890